READ THE FULL ARTICLE ONLINE
http://dx.doi.org/10.1126/science.1249783

A molecular mechanism for transmembrane signaling by the growth hormone receptor is elucidated.

RELATED ITEMS IN *SCIENCE*

J. A. Wells, A. A. Kossiakoff, New tricks for an old dimer. *Science* **344**, 703–704 (2014). DOI: 10.1126/science.1254799

Mechanism of Activation of Protein Kinase JAK2 by the Growth Hormone Receptor

Andrew J. Brooks,* Wei Dai, Megan L. O'Mara, Daniel Abankwa, Yash Chhabra, Rebecca A. Pelekanos, Olivier Gardon, Kathryn A. Tunny, Kristopher M. Blucher, Craig J. Morton, Michael W. Parker, Emma Sierecki, Yann Gambin, Guillermo A. Gomez, Kirill Alexandrov, Ian A. Wilson, Manolis Doxastakis, Alan E. Mark, Michael J. Waters*

Introduction: Class I cytokines regulate key processes such as growth, lactation, hematopoiesis, and immune function and contribute to oncogenesis. Although the extracellular domain structures of their receptors are well characterized, little is known about how the receptors activate their associated JAK (Janus kinase) protein kinases. We provide a mechanistic description for this process, focusing on the growth hormone (GH) receptor and its associated JAK2.

Rationale: We tested whether the receptor exists as a dimer in the inactive state by homo-FRET [fluorescence resonance energy transfer (FRET) between the proteins labeled with the same fluorophore] and other means. Then, to define receptor movements resulting from activation, we attached FRET reporters to the receptor below the cell membrane and correlated their movement with receptor activation, measured as increased cell proliferation. We controlled the position of the transmembrane helices with leucine zippers and mutagenesis, and we again monitored FRET and receptor activation. We used cysteine cross-linking data to define the faces of the transmembrane helices in contact in the basal state and verified this with molecular dynamics, which allowed us to model the activation process. We also used FRET reporters to monitor the movement of JAK2, and we matched this with molecular dynamics docking of the crystal structures of the kinase and its pseudokinase domains to derive a model for activation, which we then verified experimentally.

Results: We found that the GH receptor exists predominantly as a dimer in vivo, held together by its transmembrane helices. These helices are parallel in the basal state, and binding of the hormone converts them into a left-hand crossover state that induces separation of helices at the lower transmembrane boundary (hence, Box1 separation). This movement is triggered by increased proximity of the juxtamembrane sequences, a consequence of locking together of the lower module of the extracellular domain on hormone binding. Both this locking and the helix state transition require rotation of the receptors, but the key outcome is separation of the Box1 sequences. Because these sequences are bound to the JAK2 FERM (4.1, ezrin, radixin, moesin) domains, this separation results in removal of the pseudokinase inhibitory domain of one JAK2, which is blocking the kinase domain of the other JAK2, and vice versa. This brings the two kinase domains into productive apposition, triggering JAK2 activation. We verified this mechanism by kinase-pseudokinase domain swap, by changes in JAK2 FRET signal on activation, by showing association of pseudokinase-kinase domain pairs, and by docking of the crystal structures. An animation of our complete model of GH receptor activation is provided at http://web-services.imb.uq.edu.au/waters/hgh.html.

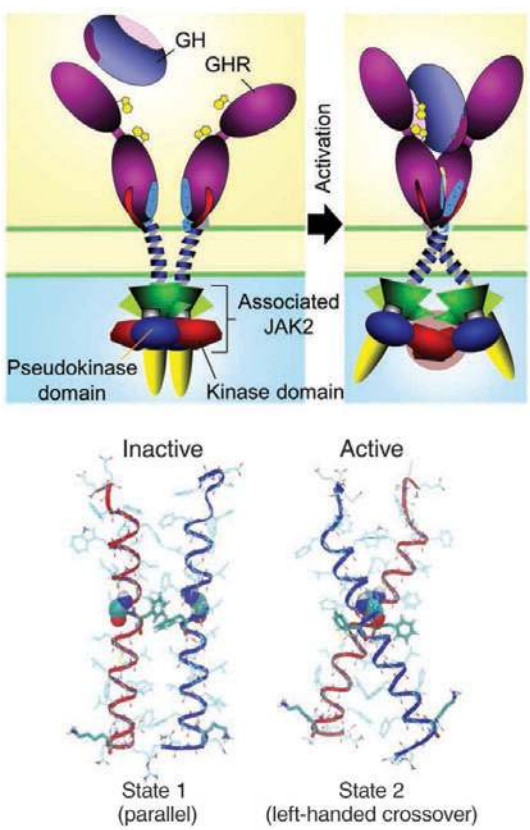

Receptor-JAK2 activation process. (**Top**) Cartoons of the GH receptor basal state (state 1, left) and the active state (state 2, right) with (**Bottom**) transmembrane helix alignments for these states derived by modeling. GHR, GH receptor.

Conclusion: The proposed mechanism will be useful in understanding the many actions of GH, which include altered growth, metabolism, and bone turnover. We expect that it may extend to other members of this important receptor family. The mechanism provides a molecular basis for understanding the oncogenic JAK2 mutations responsible for polycythemia vera and certain other hematologic disorders and may thus be of value in the design of small-molecule inhibitors of clinical applicability.

The list of author affiliations is available in the full article online.
*Corresponding author. E-mail: m.waters@uq.edu.au (M.J.W.); a.brooks@uq.edu.au (A.J.B.)
Cite this article as A. J. Brooks *et al.*, *Science* **344**, 1249783 (2014). DOI: 10.1126/science.1249783

Mechanism of Activation of Protein Kinase JAK2 by the Growth Hormone Receptor

Andrew J. Brooks,[1]* Wei Dai,[2] Megan L. O'Mara,[3] Daniel Abankwa,[1] Yash Chhabra,[1] Rebecca A. Pelekanos,[1] Olivier Gardon,[1] Kathryn A. Tunny,[1] Kristopher M. Blucher,[1] Craig J. Morton,[4] Michael W. Parker,[4,5] Emma Sierecki,[1] Yann Gambin,[1] Guillermo A. Gomez,[1] Kirill Alexandrov,[1] Ian A. Wilson,[6] Manolis Doxastakis,[2] Alan E. Mark,[1,3] Michael J. Waters[1]*

Signaling from JAK (Janus kinase) protein kinases to STAT (signal transducers and activators of transcription) transcription factors is key to many aspects of biology and medicine, yet the mechanism by which cytokine receptors initiate signaling is enigmatic. We present a complete mechanistic model for activation of receptor-bound JAK2, based on an archetypal cytokine receptor, the growth hormone receptor. For this, we used fluorescence resonance energy transfer to monitor positioning of the JAK2 binding motif in the receptor dimer, substitution of the receptor extracellular domains with Jun zippers to control the position of its transmembrane (TM) helices, atomistic modeling of TM helix movements, and docking of the crystal structures of the JAK2 kinase and its inhibitory pseudokinase domain with an opposing kinase-pseudokinase domain pair. Activation of the receptor dimer induced a separation of its JAK2 binding motifs, driven by a ligand-induced transition from a parallel TM helix pair to a left-handed crossover arrangement. This separation leads to removal of the pseudokinase domain from the kinase domain of the partner JAK2 and pairing of the two kinase domains, facilitating trans-activation. This model may well generalize to other class I cytokine receptors.

Class I cytokine receptors are key regulators of many processes, including postnatal growth, erythropoiesis, myelopoiesis, lactation, and metabolism. These receptors use the JAK-STAT (Janus kinase–signal transducers and activators of transcription) signaling pathway, which, when deregulated, becomes an important oncogenic pathway (*1*). Despite this, the molecular process responsible for activation of JAK2 tyrosine kinase by class I cytokine receptors has remained elusive.

Growth hormone (GH) and its receptor (Fig. 1) have been mechanistic exemplars for class I signaling molecules since publication of the crystal structure of the 2:1 complex of GH receptor (GHR) extracellular domains (ECDs) with the hormone (*2*). That structure and associated biophysical and mechanistic data (*3*, *4*) led to a model of receptor activation wherein hormone-induced receptor dimerization resulted in close proximity of the receptor intracellular domains (ICDs) and apposition of the activation loops within the catalytic domains of a pair of receptor-bound JAK2 protein tyrosine kinases, resulting in kinase activation (*5*). However, for the GHR and other related cytokine receptors such as the erythropoietin (EPO), prolactin, and thrombopoietin receptors, this model was superseded with the demonstration that these receptors exist largely as an inactive dimer in the absence of ligand (*6*–*11*). The transmembrane domains (TMDs) of these single-pass cytokine receptors have an important role in their constitutive dimerization, as shown by the ToxR assay for the EPO receptor (EPOR), as well as fluorescence resonance energy transfer (FRET) and coimmunoprecipitation studies with the GH and prolactin receptors. The existence of such dimers implies that a specific ligand-induced conformational change is required for signal transmission to the associated cytoplasmic JAK2 proteins.

Comparison of receptor subunit 1 in the crystal structure of the 2:1 complex of the GHR with GH bound with the unliganded crystal structure showed only minor conformational differences, implying that the signal is initiated by subunit realignment as a result of the asymmetric placement of the receptor binding sites on GH (*7*). How this realignment brings the dimeric receptor-associated JAK2 pair into productive interaction has remained elusive. Single-particle electron microscopic imaging of the homologous kinase JAK1 has not been able to resolve this issue thus far. The full crystal structure of JAK2 itself is not yet resolved (*12*). An appropriate model for JAK2 activation by its associated cytokine receptor should provide a means of removing the inhibitory pseudokinase domain from the kinase domain of JAK2 and then aligning the kinase domains for their transactivation and signal initiation. The model should also account for the observation that mutations Val^{617}→Phe^{617} (V617F) and Tyr^{613}→Glu^{613} (Y613E) (*13*), which result in constitutively active JAK2 mutants, are only active at physiological expression levels in the presence of receptor dimers (*14*, *15*). It should also encompass the finding that JAK2 binds to the juxtamembrane (JM) Box1 sequence of GHR through residues close to the end of the N-terminal FERM domain (*16*). We present a molecular model for activation of JAK2 by GH based on experimentation and molecular modeling (view animation at http://web-services.imb.uq.edu.au/waters/hgh.html).

Results

GHR TMD Interaction Supports the Role of the TMD in Constitutive Dimer Formation and the Importance of Key Residues in TMD Helix Packing

The GHR TMD is critical for ligand-independent receptor association (*7*). To characterize which interactions within the TMD contribute to constitutive GHR dimerization, we used the ToxR assay (*17*). This assay provides a colorimetric measure of TMD interactions from isolated TMDs expressed in the inner cell membrane of *Escherichia coli* (fig. S2) and has been used to demonstrate TMD association for the homologous EPOR and thrombopoietin receptor (TpoR or c-Mpl) (*10*, *18*). The ToxR assay showed that GHR TMDs self-associate (Fig. 2A), although less strongly than do the homodimeric EPOR or the leucine zipper controls, but strongly compared with the noninteracting polyalanine (alanine 16) control. The N-terminal, C-terminal, and central portions of the GHR TMD all interacted in this assay. Pro^{266} and the first glycine (Gly^{274}) of the GxxG motif [both of which are highly conserved (fig. S1)] appeared to weaken the TMD helix interaction, because interaction increased on conversion of these residues to Ile (Fig. 2, B and C). Substitution of individual residues within the TMD with alanine has negligible effect on helix interactions for these cytokine receptors (*18*), so we introduced disruptive Gly-Pro double substitutions at I272F and L282F. These substitutions decreased helix interaction [as they do for the EPOR TMD interaction, where they are thought to introduce a kink (*19*)]. Conversely, substitution of V280M with G280P had the opposite action, increasing interaction of GHR TMD helices (Fig. 2C). These results support the view that the GHR TMD helices do associate constitutively in a specific manner, but not so strongly as to preclude realignment as a result of ligand binding to the ECD.

Verification of constitutive dimer formation of GHR in mammalian cells was obtained by homo-FRET (FRET between the proteins labeled with the same fluorophore) with confocal microscopy

[1]The University of Queensland, Institute for Molecular Bioscience (IMB), St Lucia, Queensland 4072, Australia. [2]Department of Chemical and Biomolecular Engineering, University of Houston, Houston, TX 77004, USA. [3]The University of Queensland, School of Chemistry and Molecular Biosciences, St Lucia, Queensland 4072, Australia. [4]Biota Structural Biology Laboratory and Australian Cancer Research Foundation (ACRF) Rational Drug Discovery Centre, St Vincent's Institute of Medical Research, Fitzroy, Victoria 3065, Australia. [5]Department of Biochemistry and Molecular Biology and Bio21 Institute, University of Melbourne, Parkville, Victoria 3052, Australia. [6]Scripps Research Institute, La Jolla, CA 92037, USA.

*Corresponding author. E-mail: m.waters@uq.edu.au (M.J.W.); a.brooks@uq.edu.au (A.J.B.)

anisotropy analysis at the cell surface (*20*, *21*) (Fig. 2D). As controls for these experiments, we determined the FRET efficiency measured by fluorescence anisotropy of constitutive monomeric and dimeric versions of the receptor-type tyrosine-protein phosphatase α (RTPTα) transmembrane protein and compared it with that of the GHR fused to mCitrine (mCit) after residue 341, 37 residues after the Box1 sequence. For the monomeric RTPTα construct, the TMD was exchanged for the monomeric low-density lipoprotein receptor (*22*), whereas for the dimeric RTPTα construct, a constitutive disulfide bond was introduced in the extracellular domain adjacent to the TMD (*23*–*25*) (see supplementary materials). These data show that the GHR receptor exists primarily as a dimer at the surface of live cells.

Cysteine Scanning Analysis of GHR TMD Indicates Relative Orientation of Helices in the Receptor Dimer

Transmembrane domain association was verified by cysteine cross-linking of the TMD and JM residues. For these studies, a receptor construct was truncated in the intracellular domain after residue 388 and Cys^{259} was converted to Ser^{259}, resulting in a receptor without cysteines C-terminal of the lower cytokine domain. Within this construct, each amino acid from the top of the JM linker that joins the lower cytokine domain to the TMD, down to the end of the TMD (Leu^{251} to Ser^{288}), was individually mutated to cysteine, and cross-linking between receptors was examined. For these experiments, both intact cells and cell membranes were used. We cross-linked with either a cell-permeable 5 Å linker [methanethiosulfonate (MTS)] or through the formation of a disulfide bond with Cu-phenanthroline. Cross-linking with MTS in intact cells revealed dimeric and monomeric forms, with all of the N-terminal JM residues (Cys^{259} to Phe^{265}) cross-linking similarly, presumably reflecting flexibility in the absence of ligand, as shown for the EPOR (*26*). However, within the bulk of the TMD there was a helical periodicity evident in dimer formation, and when cross-linked residues were plotted on a helix wheel projection, an interaction interface (which included Ile^{272} and Phe^{273}, Ile^{275} and Phe^{276}, and Val^{280}) was apparent, with cross-linking just visible at Phe^{283} (Fig. 3, A and B). MTS has limited accessibility to residues buried deep in the bilayer where little reactive thiolate anion is present (*27*), which may account for the low efficiency of dimer formation toward the cytoplasmic side. This interface correlates well with the basal-state configuration predicted by molecular dynamics (MD) simulations (see below). The conserved GxxG motif appears not to participate in the TMD interaction in the basal state. Cross-linking of cell membranes with Cu-phenanthroline (which is less able to penetrate cell membranes) showed that cross-links could form from Thr^{258} to $Ileu^{268}$ and again from Thr^{280} to Leu^{286} at the lower TMD boundary.

We investigated the extent of cross-linking in the presence or absence of human GH (hGH) in cell membrane preparations. Increased Cu-phenanthroline–induced cross-linking of D262C, located in the JM region, was evident in the presence of hGH (Fig. 3C), although other residues did not yield consistent results. This supports the view that ligand binding increases the proximity between JM residues in this conserved membrane proximal sequence and is consistent with hGH-induced formation of disulfide dimers at the adjacent Cys 259 residue in the native receptor (*28*).

GHR Dimerization by Disulfide Bond Formation at the Extracellular JM and TMD Results in Constitutively Active Receptors

Growth hormone, like its structural homologs EPO and prolactin, has two asymmetrically placed receptor binding sites that would change the interaction geometry between the two receptor subunits on binding. To understand the nature of this change, we began with the observation that a minor fraction of the cysteine-substituted receptors described above form cross-linked dimers spontaneously in the absence of ligand (fig. S3). Hence, we could observe the activity of full-length dimerized receptor in the absence of ligand through cysteine substitution at cross-linked residues within the JM linker and upper TMD helix regions. For these experiments, we also mutated wild-type (WT) Cys^{259} to Ser^{259}. Transient expression in human embryonic kidney (HEK) 293 cells revealed that constitutive cross-linking of the GHR with cysteine substitutions between Glu^{260} and Leu^{269} is accompanied by receptor activation (measured as STAT5 Tyr^{694} phosphorylation), whereas above this, dimer formation and activation were weak. No evident dimer formation or signaling was seen with Cys^{259} converted to serine, that is, when no JM or TMD free cysteines were present (Fig. 3D). Evidently dimerization within the upper TMD or the extracellular EED sequence can initiate signaling (i.e., close apposition of the upper TMD is sufficient to initialize signaling). Accordingly, introducing two disulfide bonds by cysteine substitution at E260C and I270C resulted in even stronger receptor activation (Fig. 3D).

Controlled Dimerization of GHR Reveals that Increased Receptor Activation Correlates with an Increase in Separation of the Box1 Motifs

To better understand the steric requirements for receptor activation we substituted the GHR ECD with a leucine zipper from the transcription factor c-Jun. This allowed us to control the positioning of the TMD without compensatory movements by the ECDs. The positioning of the cytoplasmic JAK2-binding Box1 motif and its downstream sequence were monitored by placing C-terminal FRET reporters (mCit or mCFP) 37 residues below the Box1 sequence. The receptor truncation and addition of FRET reporters did not prevent

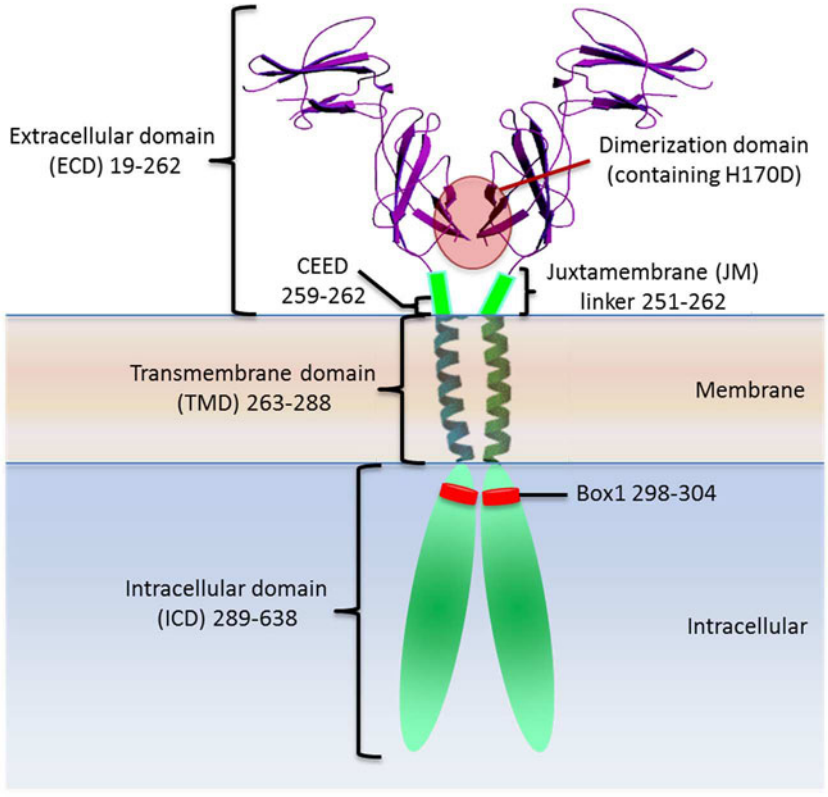

Fig. 1. Cartoon of GHR showing key features with residue numbers.

JAK2 binding, and GH addition activated JAK2 for these receptor constructs (fig. S4 and S5).

We first positioned the Jun zipper 12 residues above the presumed TMD boundary, where the GHR linker joins to the lower cytokine receptor domain. This construct results in some constitutive activation (*29*). Shortening the linker by four residues at a time revealed that the closer the Jun zipper came to the TMD, the stronger the signal was, as measured by cell proliferation (Fig. 4, A and B). The strength of the signal correlated inversely with FRET ratio; that is, signal activation was associated with separation of the Box1 and its downstream sequence (Fig. 4, C to E). Next, the Jun zipper was placed at the upper TMD boundary, and the helices were rotated by inserting one to four alanines sequentially at the junction with the TMD. There was an optimum rotational position for signal activation, with the active and inactive positions adjacent. Again, the FRET ratio indicated that separation of the Box1 and downstream sequence occurs in the active rotational position (Fig. 4, F to H). To exclude the possibility that the changes in FRET ratio resulted from reorientation of the fluorophores rather than their separation, the comparison of the 3Ala and 4Ala Jun insertion constructs was repeated with the flexible linker RSIAT (Arg-Ser-Ile-Ala-Thr) (*30*) between the fluorophores and residue 341 of the receptor. This did not influence the FRET ratio comparison, from which we conclude that the decreased FRET ratio in the active states resulted from increased distance and not fluorophore rotation (fig. S6).

Because clamping the receptors together at the upper TMD interface, either by use of the Jun zipper (Fig. 4, A to E) or through disulfide bond formation (Fig. 3D), resulted in receptor activation, we examined the role of the conserved EED acidic sequence (fig. S1) positioned therein. It seemed likely that like-charge repulsion could maintain separation of the receptors and keep the receptor in an inactive state in the absence of ligand. Repulsion could then be overcome by ligand binding, inducing closer apposition of the receptors within the constitutive dimer. We explored this hypothesis by comparing the Jun -3Ala construct with an equivalent construct in which the three alanines were reverted to the WT $E^{260}ED$ sequence. The presence of the AAA sequence compared to EED substantially increased the proliferative activity and decreased the FRET ratio below the Box1 domain (Fig. 5A), again indicating that when the receptor dimer is clamped tighter together at the upper TMD interface, the Box1 motifs separate.

If this phenomenon applied to the full-length receptor, it could act as a point of control (gate) for receptor activation. We introduced the charge reversal mutations KKR in place of the EED sequence and transduced the full-length KKR construct alone or together with the WT construct into Ba/F3 cells and measured constitutive activity. Electrostatic attraction at this position partially activated the full-length receptor (Fig. 5B). This activation was again associated with separation of the Box1 and associated sequences below the membrane, as shown with GHR constructs that contained the full ECD with mCFP/mCit reporters placed after the Box1 motif (Fig. 5C). Expression of WT-GHR or KKR-GHR individually gave similar FRET values, whereas coexpression of both constructs gave a significantly lower FRET value, again demonstrating the inverse correlation between activation and separation of the Box1 motif.

We then used the full ECD WT-GHR FRET constructs to verify that the binding of hormone alone to the receptor on intact cells also resulted

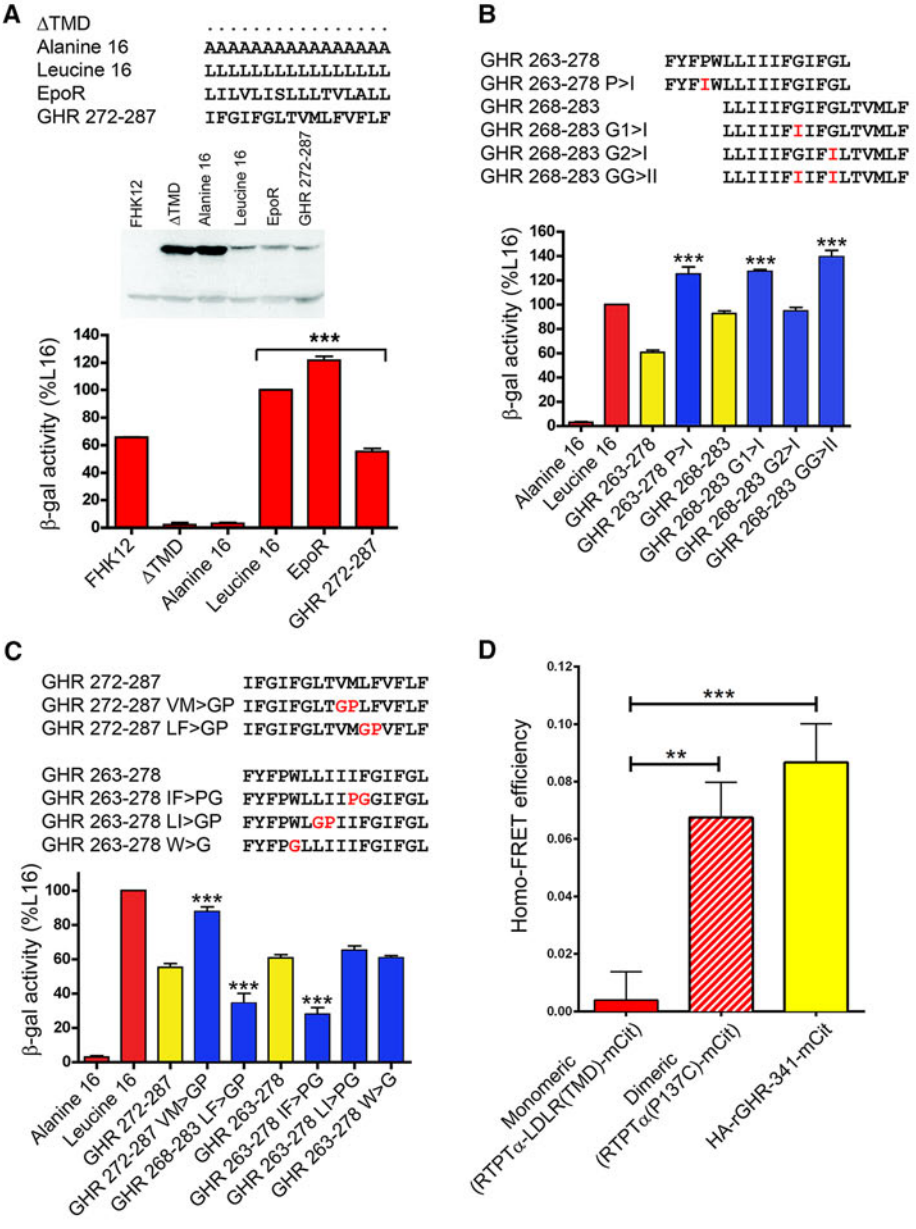

Fig. 2. Evidence of GHR dimers in cell surface membranes. (**A** to **C**) GHR TMD association shown by ToxR assay. (A) ToxR assay showing self-association of GHR and EPOR TMDs with controls showing amino acid sequences used for each TMD construct, together with a maltose-binding protein (MBP) immunoblot of the ToxR-TMD-MBP chimeric proteins expressed in FHK12 *E. coli*, which was used to normalize the β-galactosidase values in Miller units (see fig. S2 for detail). (B and C) GHR TMD sequences showing mutations introduced to perturb TMD association, as monitored in the ToxR assay (n = 4 to 17 independent experiments in triplicate, values expressed as percent L-16 value after normalization of β-galactosidase activity to MBP expression). Error bars in (A) to (C) denote average ± SEM, with one-way ANOVA and Tukey's multiple comparison post-test (**$P < 0.01$, ***$P < 0.001$ compared to test constructs). (**D**) Homo-FRET efficiency for individual mCit-labeled proteins using confocal microscopy anisotropy analysis at the surface of live mammalian cells. Controls were constitutive monomeric and dimeric versions of the RTPTα transmembrane protein.

in a decreased FRET ratio with membrane extracts from these cells (Fig. 5D). Introduction of the GHR D170H mutation (often referred to as D152H using numbering of the mature protein), which results in GH-insensitive Laron dwarfism (*31*), into these FRET constructs prevented the decrease in FRET seen with WT receptor in response to GH binding (Fig. 5D). The decrease in FRET ratio induced by WT GH was not seen with the clinical GH antagonist G120R hGH, and this also blocked the decrease in FRET ratio induced by WT GH (Fig. 5D).

Previous observations that hormone binding to GHR produced a transient increase in FRET signal (*32*) may have resulted from FRET reporters being placed at the C terminus. Given the relative immobilization of receptor-bound JAKs below the TMD, the lower cytoplasmic domains must move toward the JAKs for tyrosine phosphorylation to occur. This would be facilitated by an unstructured cytoplasmic domain, as is known to occur in the JAK1-gp130 couple (*33*).

Role of Lys^{289} at the GHR TMD-ICD Boundary in Receptor Activation

The data presented above are consistent with a gating mechanism at the upper TMD boundary that holds the receptors apart, minimizing activation in the absence of ligand. We investigated whether there are residues that hold the submembrane sequences together in the inactive state as there are in the TpoR, in which mutations within the conserved sequence above the Box1 domain result in constitutive activation and myeloproliferative neoplasms (*34*). Alanine substitution within the equivalent conserved SKQQRIK sequence (fig. S1) in the GH receptor revealed that conversion of the first lysine residue (Lys^{289}) to alanine resulted in increased signaling (Fig. 5, E and F). The equivalent K507A mutant in TpoR also showed increased activation (*30*). Again, for K289A GHR, the submembrane FRET reporters indicate increased separation of the Box1 sequences (Fig. 5E) through movement of the JM α-helical sequence (*35*).

Active and Inactive Dimer Orientations Identified by Molecular Simulations of GHR TMDs

To understand the above experimental data in terms of a molecular model, we undertook extensive in silico modeling of the hGHR TMD helix dimers, initially assuming the helices were in a vacuum. Searches of helix rotation angles for both right- and left-handed crossing angles predicted a helix alignment corresponding to the cross-link data (Fig. 3A), with interactions between Phe^{276}

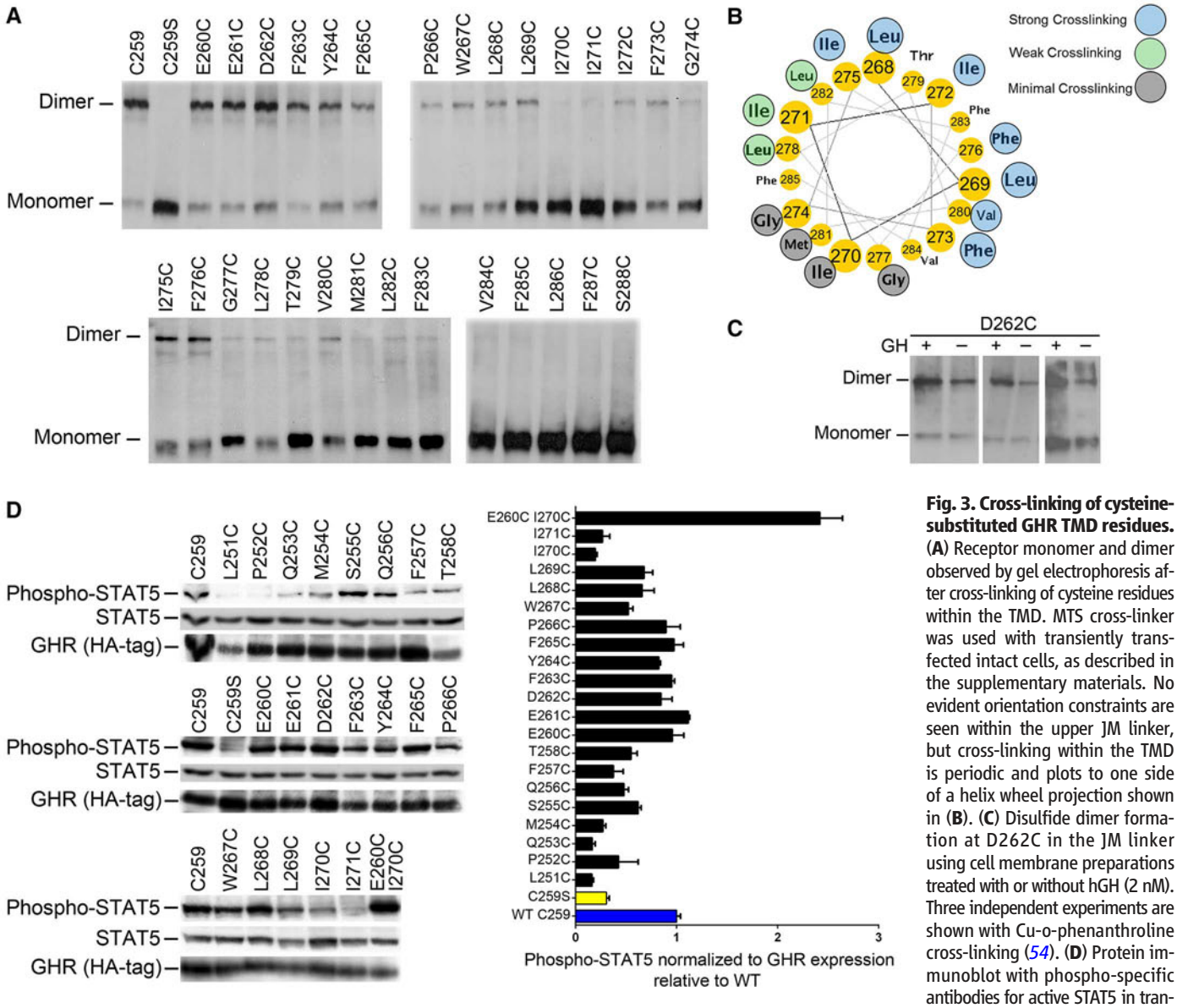

Fig. 3. Cross-linking of cysteine-substituted GHR TMD residues. (**A**) Receptor monomer and dimer observed by gel electrophoresis after cross-linking of cysteine residues within the TMD. MTS cross-linker was used with transiently transfected intact cells, as described in the supplementary materials. No evident orientation constraints are seen within the upper JM linker, but cross-linking within the TMD is periodic and plots to one side of a helix wheel projection shown in (**B**). (**C**) Disulfide dimer formation at D262C in the JM linker using cell membrane preparations treated with or without hGH (2 nM). Three independent experiments are shown with Cu-o-phenanthroline cross-linking (*54*). (**D**) Protein immunoblot with phospho-specific antibodies for active STAT5 in transiently transfected HEK293 cells. Levels of receptor expression are shown by corresponding blots for HA-tagged hGHR. The histogram shows the pSTAT5 level normalized to receptor protein expression for three replicate experiments [mean ± SEM (error bars)].

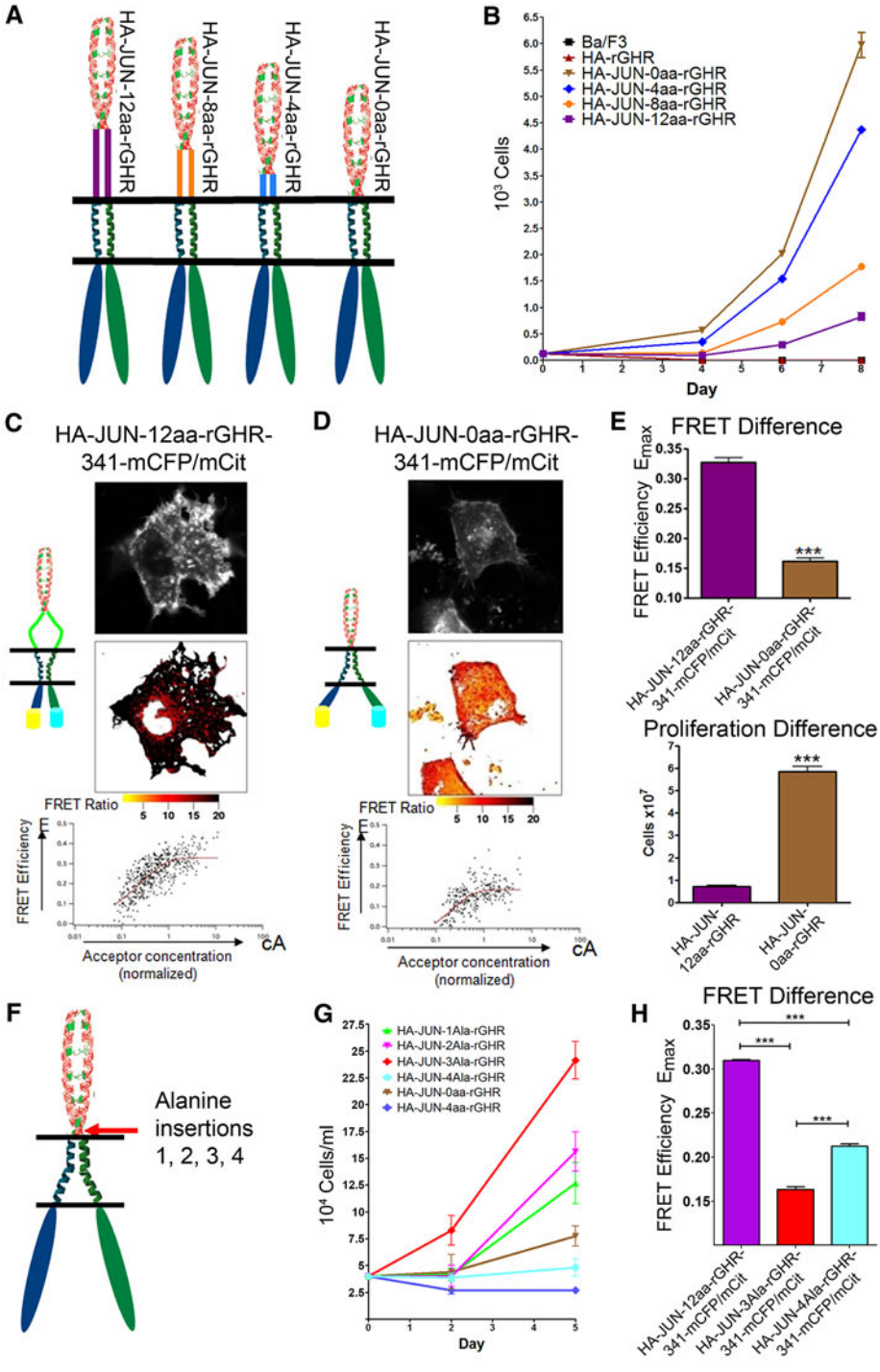

Fig. 4. Replacement of ECD with Jun zippers to enable analysis of orientational constraints in constitutive signaling by GHR. (**A**) Shortening of the linker between the Jun zipper and the TMD results in (**B**) increased receptor activation in Ba/F3 cells stably expressing Jun fusion constructs (measured as increased cell number). (**C** and **D**) FRET efficiency images (top image, total fluorescence; lower image, FRET efficiency, where darkest is highest FRET efficiency, see code bar) by live-cell confocal microscopy, together with fluorescence-activated cell sorting (FACS) FRET analysis for individual cells showing an inverse relation between cell proliferation (measured as in Materials and Methods, with cell number shown at day 8) and FRET ratio for these constructs (**E**). (**F**) Rotation of the Jun-clamped TMD by insertion of one to four alanines into the HA-JUN-0aa-rGHR construct reveals an optimum orientation of the TMD helix for signaling, measured as cell proliferation (**G**), and this correlates with decreased FRET reporter signal below the TMD (**H**). Error bars in (B), (E), (G), and (H) denote SEM. ***$P < 0.001$.

and Phe^{283} (lowest free energy, cluster 1, fig. S7A). The rather different chicken GHR sequence was predicted to give a similar alignment (fig. S7C).

To understand the dynamics of receptor activation, we used MD simulations to model the behavior of the TMDs in a lipid bilayer (Fig. 6, A and B, and supplementary materials). A coarse-grained representation of the peptide, lipids, and solvent (*36*) was used to obtain the free-energy profile as a function of distance (PMF) between two TMDs by exhaustive Monte Carlo simulations of 128 replica pairs for a range of separations between the centers of mass of the helices (*37*). The fact that the PMF has a deep minimum at a separation of 0.7 to 0.8 nm with a predicted free energy of binding around 10 kcal/mol supports the finding that two TMDs interact strongly with minimal free monomer present (Fig. 6B).

We sought measures to characterize our modeling data such as the crossing angle Ω between the helix axes, We mapped the contacts between the two helices as they approach within a lipid bilayer (Fig. 6C). Helices tilt and interact first when the lateral separation of the centers of mass is ~2 nm. Repulsive interactions at the N termini result in formation of an initial contact at the C termini. Subsequently, the TMDs follow a path that maximizes interactions between the Phe residues and Thr-Thr hydrogen bonding. This initially leads to an essentially parallel dimer (state 1 in Fig. 6D) with a low Ω value but with many interactions. Closer approach of the helices (as could result from hormone binding) leads to a close-packed structure (state 2 in Fig. 6E) with increased tilting and Ω, resulting in a left-handed crossover dimer with increased separation at the C terminus (see below). Both states 1 and 2 lie within the energy minimum (Fig. 6B), indicating a relatively facile state 1–to–state 2 transition. This transition has been observed for other TMDs using coarse-grained and atomistic simulations in simpler environments (*38*, *39*). GHR TMDs form the left-handed dimer by rotating Phe^{276} and Phe^{283} out of the interface. Importantly, right-handed essentially parallel dimers at close separation readily rearrange to left-handed dimers (state 2) by substitution of disulfide bonds at Glu^{260} and Ile^{270} (Fig. 7, A and B), correlating with the constitutive receptor activation of such dimers (Fig. 3D). This is analogous to the activation seen by moving the Jun zipper down onto the cell surface (Fig. 4B).

To better identify structures correlated to activity, we needed to compare our predictions with mutation and cross-linking experiments. Therefore, atomistic models of helical TMDs were superimposed onto the structures from the coarse-grained simulations and subjected to MD in large lipid-bilayer systems. For state 1, three structures were each simulated for 0.3 μs. Figure 6D shows a snapshot of one such dimer (state 1), together with an analysis of the separation between specific residues for which cysteine substitutions had been performed for each of the three trajectories. All three dimers fluctuated somewhat but maintained a separation of between 0.9 and 1.2 nm,

slightly tilted relative to the normal of the bilayer and in a parallel arrangement with low Ω. These dimers are characterized by extensive interactions between Phe residues and appear to be stabilized by Lys^{289}, which anchors the lower C termini at the water–hydrophobic region boundary. The predicted sulfur-sulfur separation distances closely resembled the experimental cross-link pattern seen with cysteine–cross-linking experiments in the absence of ligand, supporting state 1 as the inactive state. Gly^{274} is far from the helix interface in the absence of hormone.

A 0.7-μs full atomistic simulation for the most stable dimer predicted by the simpler coarse-grain model (state 2) showed that it remained helical throughout the simulation (Fig. 6E). Backbone atoms presented small fluctuations with an overall lateral separation of 0.8 nm. Helices tilted,

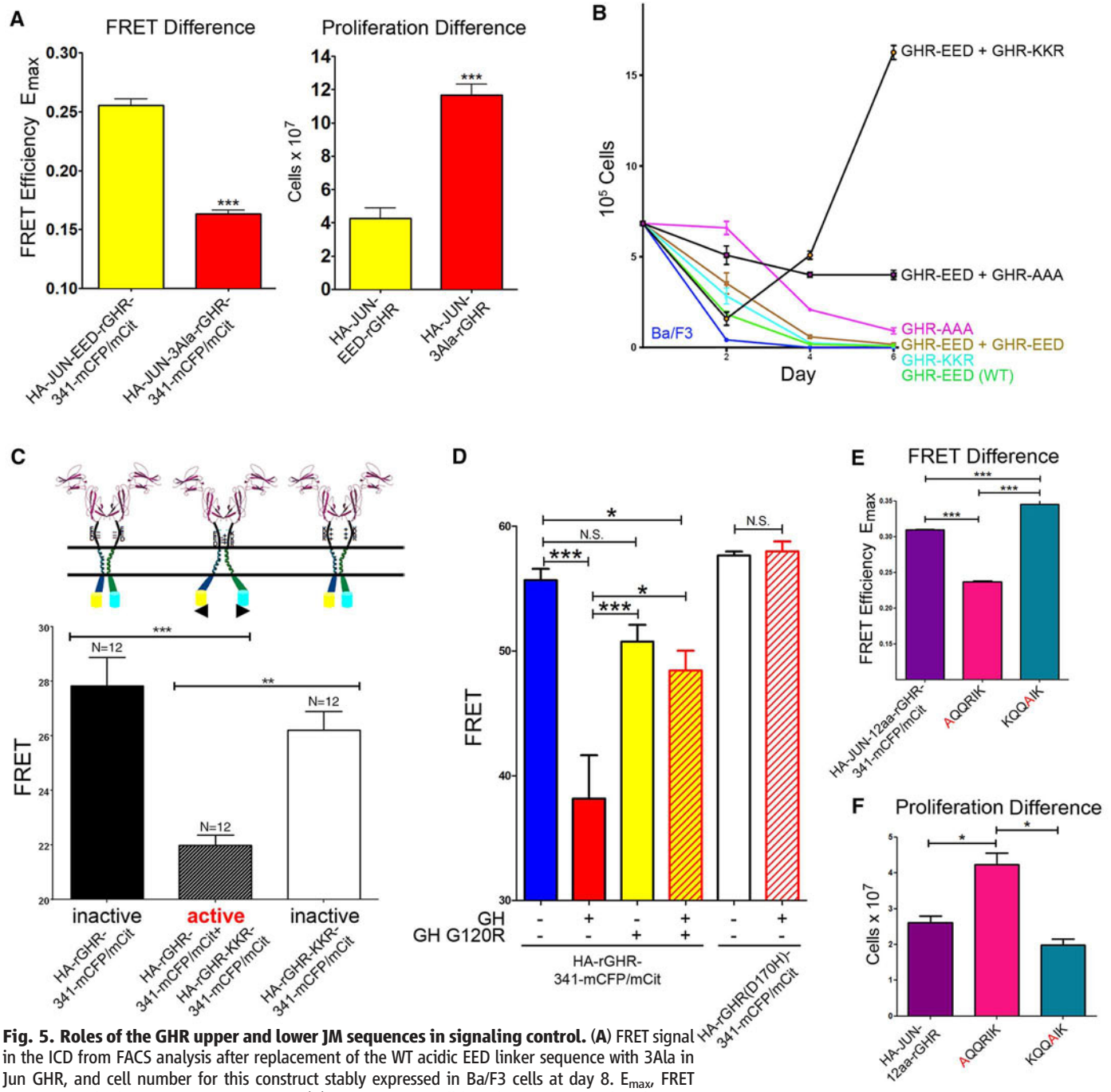

Fig. 5. Roles of the GHR upper and lower JM sequences in signaling control. (**A**) FRET signal in the ICD from FACS analysis after replacement of the WT acidic EED linker sequence with 3Ala in Jun GHR, and cell number for this construct stably expressed in Ba/F3 cells at day 8. E_{max}, FRET efficiency at high acceptor concentration. (**B**) Expression of full-length GHR in transduced Ba/F3 cells with WT GHR or GHR with the E^{260}ED residues substituted to AAA or KKR. (**C**) Decreased FRET with membrane preparations when FRET reporters are placed below Box1. This activation correlates with increased proliferation. N, number of replicates. (**D**) FRET ratio in membrane preparations from transiently expressed rGHR-reporter constructs in HEK 293T cells treated with or without hGH (5 nM) or with G120R hGH (500 nM). Cells were also incubated with 500 nM G120R hGH for 10 min before treatment with 5 nM hGH. The GHR D170H Laron mutant showed no FRET change upon GH addition. N.S., not significant. (**E** and **F**) Substitution of Lys^{289} with Ala promotes proliferative signaling in stably expressing Jun GHR Ba/F3 cells (shown for proliferation assay at day 3), and this correlates with decreased FRET from FACS analysis from reporters placed below Box1. ANOVA with Tukey post hoc test, $*P < 0.05$, $***P < 0.001$. Error bars in all panels denote SEM.

rotated, and packed against Gly^{274} with a separation of substituted cysteines distinctively different from those obtained in experimental data for the inactive receptor. When the inactive state (Fig. 6D) was compared with the left-handed crossover form (Fig. 6E), separation between the C termini was increased (evident in the cysteine substitution sulfur-sulfur distances). The increased separation parallels our finding that activity correlates with higher separation of the C termini, as monitored by FRET. Moreover, in the proposed active state 2 form, the N-terminal Trp^{267} sits favorably at the membrane interface, facing outward to favor association, whereas the C-terminal Lys-^{289} is in an unfavorable configuration for helix interaction (allowing greater separation), consistent with nuclear magnetic resonance studies using model peptides (*40*). Thus, the model can explain how alanine substitution of Lys-^{289} promotes the left-handed dimer form, correlating with the increased activation seen on conversion of Lys-^{289} to Ala (Fig. 5, E and F).

We constructed a chimeric model in which the proposed TMD dimer configurations were joined to the crystal structure of the human GH:ECD receptor complex [Protein Data Bank (PDB) ID: 3HHR]. Missing residues were generated with

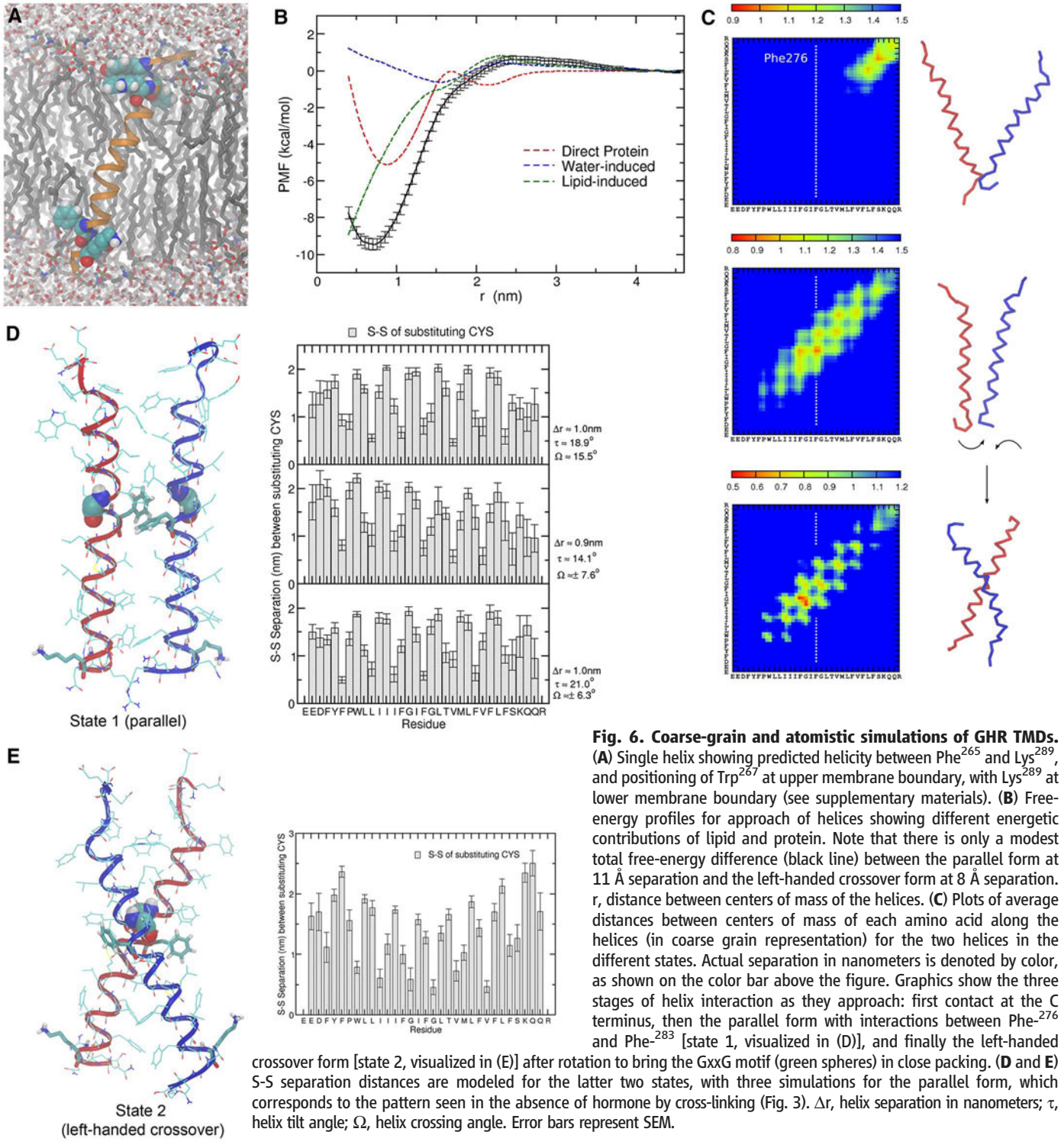

Fig. 6. Coarse-grain and atomistic simulations of GHR TMDs. (**A**) Single helix showing predicted helicity between Phe^{265} and Lys^{289}, and positioning of Trp^{267} at upper membrane boundary, with Lys^{289} at lower membrane boundary (see supplementary materials). (**B**) Free-energy profiles for approach of helices showing different energetic contributions of lipid and protein. Note that there is only a modest total free-energy difference (black line) between the parallel form at 11 Å separation and the left-handed crossover form at 8 Å separation. r, distance between centers of mass of the helices. (**C**) Plots of average distances between centers of mass of each amino acid along the helices (in coarse grain representation) for the two helices in the different states. Actual separation in nanometers is denoted by color, as shown on the color bar above the figure. Graphics show the three stages of helix interaction as they approach: first contact at the C terminus, then the parallel form with interactions between Phe-^{276} and Phe-^{283} [state 1, visualized in (D)], and finally the left-handed crossover form [state 2, visualized in (E)] after rotation to bring the GxxG motif (green spheres) in close packing. (**D** and **E**) S-S separation distances are modeled for the latter two states, with three simulations for the parallel form, which corresponds to the pattern seen in the absence of hormone by cross-linking (Fig. 3). Δr, helix separation in nanometers; τ, helix tilt angle; Ω, helix crossing angle. Error bars represent SEM.

the Modeller program (http://salilab.org/modeller/about_modeller.html). The overall best configuration based on Modeller's objective function for the linking amino acids (Fig. 7C) shows a good fit between the ECD positioning and the state 2 configuration and places the two Cys^{259} residues in close enough proximity to form a disulfide bond, as shown experimentally after GH addition (*28*). We could also identify potential interreceptor hydrogen bonds in the linker that could assist in stabilizing the active configuration, between Glu^{260} of receptor 1 and the amide of Trp^{267} in receptor 2, as well as between the backbone carbonyl of Phe^{257} and amide of Glu^{260} in receptor 2. The ECDs without the hormone were attached to the parallel TMD (state1). This simulation produced rotation of the ECDs, as described for isolated ECDs (*41*). In that simulation, the linker regions sat on the membrane, although the ECD domains did not separate. This observation is consistent with our inability to cross-link receptors above Cys^{259} efficiently in the basal state. Potentially, this is related to repulsion between the acidic EED sequences.

A Model for GHR Activation

The above findings are consistent with a model of receptor activation in which binding of GH through its asymmetrically placed binding sites (*2*) realigns the two receptors by relative rotation [as evident in MD simulations (*41*)] and, together with elevation of receptor 1, locks the two dimerization domains in the ECD closely together. This locking is necessary for signal transduction (*42*, *43*) and brings the upper TMD sequences close together by overcoming the electrostatic repulsion of the EED sequences. Closer apposition of the adjacent juxtamembrane sequences is presumably the reason for resistance to proteolytic attack on the receptor when GH is bound, in contrast to its sensitivity when the G120R hGH antagonist is bound (*44*). Closure of the upper TMD would promote the transition to the left-handed TMD form, with increased separation of the Box1 sequences.

A Model for JAK2 Activation by GH

Separation of the JAK2-binding Box1 sequences can provide a mechanism for JAK2 activation.

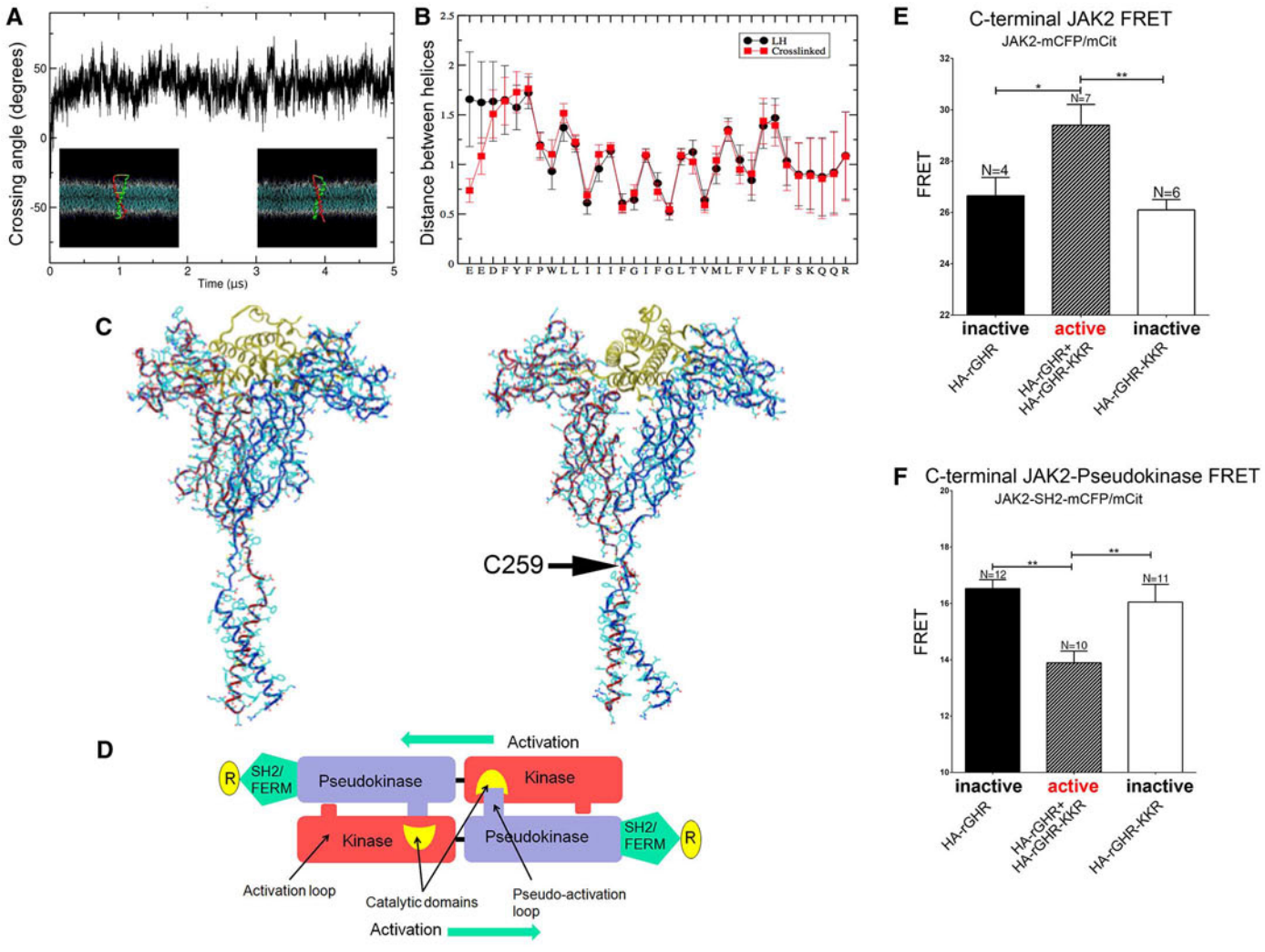

Fig. 7. Validation of the GHR homology model. Repositioning of JAK2 observed by FRET. (**A**) Disulfide bonding between cysteines substituted at Glu^{260} and Ile^{270} rapidly converts state 1 to state 2 in MD simulations, correlating with constitutive activation seen experimentally. (**B**) MD of the active disulfide dimer: Distances in nanometers between backbone residues of each amino acid to the corresponding residue of the other helix overlay closely on those for state 2. Error bars represent SEM. (**C**) Full-length simulations. The best model of the JM linker joined to the hGH:ECD receptor complex crystal structure (PDB ID: 3HHR) is shown. Note the proximity of Cys^{259} residues, which form a disulfide bond on addition of ligand. Between linkers, there are also two potential hydrogen bonds that could stabilize this conformation (see text). (**D**) Diagram of JAK2 dimer showing proposed movement of kinase and pseudokinase domains after receptor TMD separation in state 2. (**E** and **F**) FRET ratio measurements with activated receptor (WT + KKR charge reversal mutant as in Fig. 5, B and C) and KKR or WT receptor alone, showing convergence of kinase domains and separation of pseudokinase domains on activation. Error bars indicate SEM. $^{*}P < 0.05$, $^{**}P < 0.01$.

We have considered how such a separation might occur within a receptor dimer containing a JAK2 molecule bound to each receptor, given the finding that even constitutively activated oncogenic JAK2 mutants V617F, L611S, and Y613E require the presence of receptor for activity (*14*, *15*); that is, the receptors need to be present to correctly appose the kinase domains for efficient transactivation. If the kinase domain of one JAK2 molecule is inhibited by the complementary pseudokinase domain of the second JAK2 and vice versa, then moving the JAK2 molecules apart in a sliding motion would remove the pseudokinase domain inhibitions and bring the kinase domains into productive proximity (Fig. 7D and animation at http://web-services.imb.uq.edu.au/waters/hgh.html).

Activation of JAK2 by GH Through Removal of Trans-Inhibition

To provide experimental evidence for this model, we placed FRET reporters (mCFP or mCit) at strategic locations within JAK2 and then compared the FRET ratios when cells were transduced with WT rabbit GHR (rGHR), rGHR that had the EED-to-KKR substitution, or both. This strategy allowed measurement of FRET ratios when all receptors were fixed in an inactive basal state or when a subset of receptors were fixed in an active orientation. FRET reporters were placed at the C terminus of JAK2, to monitor movement of the catalytic domains, or C-terminal to the SH2 domain at Asn^{533}, in place of the pseudokinase domain. Reporter pairs were cotransfected (or transfected separately for FRET calculations) into HEK293T cells with the rGHR expression plasmids. Washed membrane preparations were then prepared from these cells (to reduce the background signal from free JAK2), and FRET ratios were determined. Although FRET ratio changes were small (Fig. 7, E and F), they were consistent. The small changes in FRET may result from

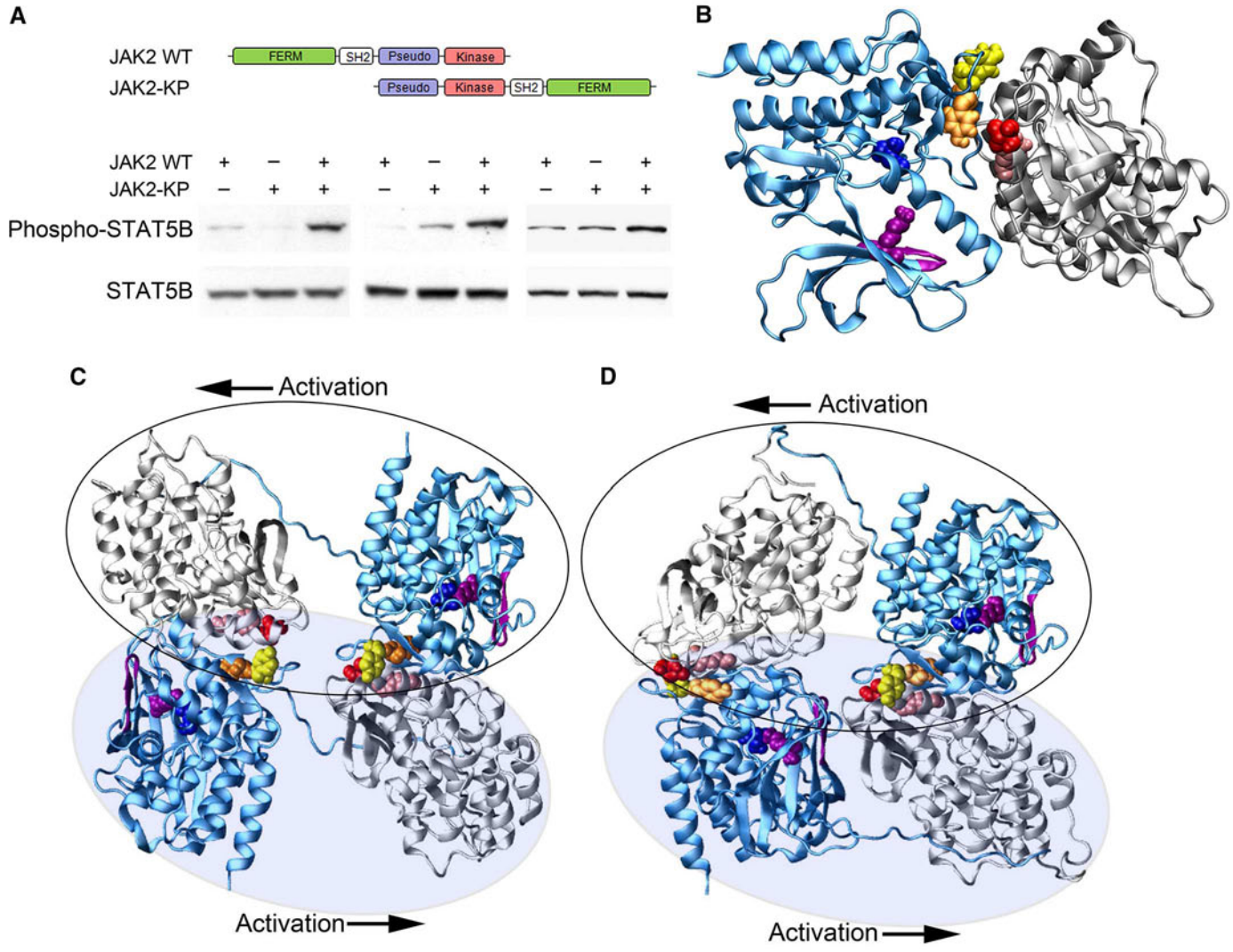

Fig. 8. JAK2 domain swap. (**A**) Diagram of JAK2 domain swap construct. Immunoblots showing constitutive activation of JAK2 when kinase and pseudokinase domains are swapped and the domain swap is cotransfected with WT JAK2. Result of three independent experiments shown with identical total JAK2 plasmid quantity. (**B**) The pseudokinase-kinase domain interface in the inactivated state after 40 ns of MD. The pseudokinase and kinase domains are shown in gray and blue ribbons, respectively. The following key residues are shown in space-fill representation: F595 (pink: required for V617F constitutive activation), V617 (red: mutation causing constitutive activation), substrate binding site D976 (blue), and activation loop phosphorylation residues Y1007 (yellow) and Y1008 (orange). The adenosine triphosphate (ATP) binding site and catalytic K882 are shown in purple ribbons and space-fill, respectively. View of the dimer interface from below shows that the ATP binding site is located in the center of residues implicated in constitutive activation. The dimer conformation derived from MD simulations can be used to construct two tetrameric orientations that fulfill the experimental data: (**C**) a stacked tetramer (**D**) or an inverse stacked tetramer, with each JAK2 circled. Arrows show proposed direction of movement induced by receptor separation below TMD, removing pseudokinase domain inhibition and bringing the kinase domains in proximity.

FRET observed between three receptor interaction possibilities when the KKR mutant is expressed with the WT receptor: WT-WT (inactive), KKR-KKR (inactive), and WT-KKR (active). The significant increase in FRET ratio for the C-terminal reporters (Fig. 7E) is consistent with the requirement for the kinase domains to transactivate, whereas the reporters positioned in the location of the pseudokinase domain [i.e., C-terminal to the SH2 domain (Fig. 7F)] showed a decreased FRET ratio in accord with the model (Fig. 7D) and animation.

To further substantiate our JAK2 activation model, the kinase and pseudokinase domains were swapped (JAK2-KP) and then transfected together with a WT JAK2 construct and the GH receptor into JAK2-deficient human fibrosarcoma γ2A cells. Our model would predict constitutive JAK2 activity only when these two JAK2 constructs are together, but not for either alone. Indeed, STAT5 phosphorylation by JAK2 was increased when WT JAK2 and JAK2-KP were present [in each experiment, the total amount of JAK2 transfected was the same (Fig. 8A)]. Overexpression of JAK2 leads to constitutive activation (*45*), which explains why some activated STAT5 is detectable when each JAK2 construct is transfected separately.

Molecular Modeling of the Interaction of the JAK2 Kinase and Pseudokinase Domains

Currently, only the crystal structures of individual JAK2 kinase and pseudokinase domains are known (*46*, *47*). To test if the proposed model is compatible with these structures, we docked the pseudokinase and kinase domain structures with the HADDOCK program. The resulting equilibrated dimer after 40 ns of unrestrained MD simulations (Fig. 8B) represents the interaction between the kinase of one molecule and the pseudokinase domain of another. In particular, the docked structures predict a close complementary interaction between the opposing kinase and pseudokinase domains. The structure shows proximity between the activation loops and Val^{617} in the pseudokinase domain, which, when mutated, results in constitutive activation and oncogenesis. To make a model of the complete complex, we placed docked kinase and pseudokinase pairs in alternative orientations with another pair, and the cognate domains of each JAK2 were joined with their 30-residue interdomain linker. The two orientations and their movements were consistent with our experimental results (Fig. 8, C and D).

We verified that the pseudokinase-kinase pair can associate with a second such pair using AlphaScreen technology (fig. S9, A to C) based on cell-free expression of N-terminal enhanced green fluorescent protein (eGFP) or C-terminal mCherry-Myc tagged pairs. We supported this with single-molecule brightness coincidence results consistent with dimerization of GFP-tagged pseudokinase-kinase pairs in cell-free conditions (fig. S9D). Although the separate kinase domains do not associate under these conditions, the pseudokinase-kinase pairs do associate effectively in trans (fig. S9, E and F).

Discussion

We propose a mechanism for activation of JAK2 by the growth hormone receptor, an archetypal class I homomeric cytokine receptor. The receptor exists primarily as a constitutive dimer with its TMDs held in an inactive orientation in the absence of hormone. Activation of the receptor is associated with the separation of the membrane proximal signaling domains below the TMD, as assessed by FRET, and is consistent with MD modeling of the TMD.

In formulating a model to explain the increased separation of Box1 sequences on ligand binding, we were cognizant of our earlier finding that locking together of the ECD dimerization domains of the membrane proximal cytokine receptor module by specific hydrogen bonds and electrostatic bonds is essential for GH signaling (*42*). Based on MD modeling (*41*), this locking requires a relative rotation of receptor subunits of ~40°, and disruption of this lock with the D170H mutation results in GH-insensitive (Laron) dwarfism (*1*). We had proposed that this locking resulted in activation of the receptor by relative rotation of the TMDs that was transmitted to the JAK2 binding Box1 sequence to allow contact of their catalytic kinase domains (*7*). However, when we introduced alanine insertions in the upper TMD of full-length receptor, we observed only weak receptor activation, indicating that some other ligand-induced movement was necessary for full activation.

We explored the geometry of activation by clamping the receptor signaling units (TMD and cytoplasmic domain) together and found that bringing the clamp down to the membrane surface gave the strongest activation, although concurrent insertion of alanines at the upper TMD boundary did show an optimum rotational position within that clamped receptor. Moreover, cross-linking at the EEDF sequence just above the TMD activated the receptor in an analogous manner to the Jun zipper clamp. Similar cross-linking results have been reported for the full-length EPOR (*26*, *48*), and an optimum rotational position for activation has been reported for both EPOR (*49*) and TpoR (*50*). These findings suggest a common mechanism within related class I receptors involving both an optimum rotational position and the need to closely appose the upper JM sequences for activation, resulting in a tilt-and-twist movement of the TMDs. This is supported by the finding that the TMD and ICD of the granulocyte colony-stimulating factor receptor and GHR, both class I cytokine receptors, can be interchanged to produce signaling-competent receptors (*51*). This result implies that the conserved GxxG sequence of the GHR TMD is not necessary for receptor activation.

Our activation model requires separation of the Box1 motifs, resulting in activation of JAK2 bound by its FERM domain to the lower JM segment of each receptor. Current models of JAK2 assume that it exists as a monomer, where each JAK2 is autoinhibited by its own pseudokinase domain in the basal state (*52*). However, other studies (*14*, *15*) show that constitutively active JAK2 point mutations require a receptor dimer to be active at physiologic levels. The original JAK2 structural model (*53*) has been superseded by the crystal structures of the JAK2 kinase and pseudokinase domains. We used these to determine if two kinase domains and two pseudokinase domains could pair in a complementary fashion such that an increased distance between the receptors and their attached JAK2 would slide the pseudokinase domains away from the kinase domains of their opposing counterpart and bring the two kinase domains together for trans-activation. We found optimized docked solutions that allowed this interaction, and we also located key residues known to be associated with constitutive activation of JAK2 (e.g., in myeloproliferative disorders) in the interface between the inhibitory pseudokinase domain and its kinase domain complement in the basal state. By placing FRET reporters either at the C terminus (kinase domain) or in place of the pseudokinase domain, we were able to show experimentally that the FRET ratio for the pseudokinase domains decreased on receptor activation, whereas the ratio for the catalytic domains increased, supporting a model in which the domains slide apart. Further, by exchanging the kinase and pseudokinase domains, we obtained strong experimental support for our model. When this domain-reversal mutant was expressed together with WT JAK2, constitutive activity was evident. Finally, we showed with single-molecule fluorescence brightness and AlphaScreen technology that the pseudokinase-kinase domain pair can associate in trans with another such pair. We anticipate that these findings will provide valuable insights into the design of cytokine receptor therapeutics and will facilitate understanding of relevant cytokine-related genetic disorders.

Materials and Methods

ToxR Assay of TMD Interaction

This well-validated assay provides a means for testing the interaction of transmembrane helices that are placed in the inner membrane of bacteria. ToxR assays were performed essentially as previously described (*17*), using regions of the GHR TMD described in the Results section. See fig. S2 for the principle of this assay.

Cysteine Cross-Linking Studies

A series of N-terminal hemagglutinin (HA)–tagged hGHR mutants in pcDNA3.1 was constructed using QuikChange mutagenesis (Agilent Technologies), where every residue from Pro^{252} to Ser^{288} was converted to a cysteine after converting Cys^{259} to serine. Two sets of these mutants were used: either truncated at residue 389 (for cross-linking studies) or full-length GHR (for STAT5 activation studies). These mutants were used for cross-linking according to Guo *et al*. (*54*) and for

immunoblotting or signal activation studies as detailed in the supplementary materials.

Analysis of Proliferative Signal from GHR Constructs

The strength of constitutive proliferation signal from GHR constructs was assessed by starving Ba/F3 cells overnight in Ba/F3 starve media (see supplementary materials). Cultures were then counted using a Scepter with 40-μM sensors (Millipore) and seeded at equal concentrations into three flasks for each sample and cultured in starve media. Cell concentration was subsequently counted on following days and plotted as shown.

FRET Analysis

FRET measurements, using expression constructs detailed in the supplementary materials, were performed on single cells by confocal microscopy and flow cytometry essentially as previously described (*55*). Membrane extracts and FRET analysis with a fluorescence plate reader were essentially as described previously and detailed in the supplementary materials. Live cell membrane homo-FRET methods are described in the supplementary materials.

Signaling Analysis of JAK2 Cotransfected with Kinase-Pseudokinase Domain Swap JAK2

Expression constructs for WT murine JAK2 and for JAK2 with the kinase domain and pseudokinase domain swapped [referred to as JAK2-KP corresponding to (Met^{1}-Ile^{540})-(Asp^{840}-Ala^{1132})-(Gly^{831}-Arg^{839})-(Asn^{542}-Gly^{834})] were constructed as described in the supplementary materials. JAK2-deficient (and STAT5-deficient) γ2A cells (a gift from G. Stark, Imperial Cancer Research Fund, London) were transfected with expression plasmids for hGHR, STAT5B, and either WT-JAK2 or JAK2-KP separately, or WT-JAK2 and JAK2-KP cotransfected. In each set of experiments in which P-STAT5 signal from cotransfected WT-JAK2 and JAK2-KP was compared with each JAK2 construct transfected separately, the total amount of JAK2 transfected was identical. Details are given in the supplementary materials.

JAK2 Interface Model

To construct a model of the interface between the pseudokinase and kinase domains of neighboring subunits, the crystal structures of the JAK2 pseudokinase (PDB ID: 4FVP) and kinase (PDB ID: 2B7A) domains were docked using the HADDOCK Web server with distance constraints between Tyr^{1007} of the kinase domain and both Phe^{595} and Val^{617} of the pseudokinase domain. The docked model was then refined by simulating it for 40 ns in water. (Full details are given in the supplementary materials.) The actual interface between the two consecutive kinase-pseudokinase pairs is not known. To generate possible arrangements of JAK2 dimers that are consistent both with the 30–amino acid linker sequence and with our experimental data, a second copy of the MD conformation of the pseudokinase–kinase domain dimer was positioned adjacent to the original pair. That this arrangement was possible was confirmed by modeling in the missing linker region. Note that although the proposed arrangement is possible, the model does not preclude the possibility of other arrangements being consistent with the data.

Statistics

One-way analysis of variance (ANOVA) was undertaken with Tukey's multiple comparison test, whereas for comparisons of two groups, only unpaired Student's *t* test was used. Significance was shown as $*P < 0.05$, $**P < 0.01$, and $***P < 0.001$, with SEM.

References and Notes

1. A. J. Brooks, M. J. Waters, The growth hormone receptor: Mechanism of activation and clinical implications. *Nat. Rev. Endocrinol.* **6**, 515–525 (2010). doi: 10.1038/nrendo.2010.123; pmid: 20664532
2. A. M. de Vos, M. Ultsch, A. A. Kossiakoff, Human growth hormone and extracellular domain of its receptor: Crystal structure of the complex. *Science* **255**, 306–312 (1992). doi: 10.1126/science.1549776; pmid: 1549776
3. B. C. Cunningham *et al.*, Dimerization of the extracellular domain of the human growth hormone receptor by a single hormone molecule. *Science* **254**, 821–825 (1991). doi: 10.1126/science.1948064; pmid: 1948064
4. G. Fuh *et al.*, Rational design of potent antagonists to the human growth hormone receptor. *Science* **256**, 1677–1680 (1992). doi: 10.1126/science.256.5064.1677; pmid: 1535167
5. J. A. Wells, Binding in the growth hormone receptor complex. *Proc. Natl. Acad. Sci. U.S.A.* **93**, 1–6 (1996). doi: 10.1073/pnas.93.1.1; pmid: 8552582
6. J. Gent, P. van Kerkhof, M. Roza, G. Bu, G. J. Strous, Ligand-independent growth hormone receptor dimerization occurs in the endoplasmic reticulum and is required for ubiquitin system-dependent endocytosis. *Proc. Natl. Acad. Sci. U.S.A.* **99**, 9858–9863 (2002). doi: 10.1073/pnas.152294299; pmid: 12105275
7. R. J. Brown *et al.*, Model for growth hormone receptor activation based on subunit rotation within a receptor dimer. *Nat. Struct. Mol. Biol.* **12**, 814–821 (2005). doi: 10.1038/nsmb977; pmid: 16116438
8. K. F. Kubatzky *et al.*, Self assembly of the transmembrane domain promotes signal transduction through the erythropoietin receptor. *Curr. Biol.* **11**, 110–115 (2001). doi: 10.1016/S0960-9822(01)00018-5; pmid: 11231127
9. S. L. Gadd, C. V. Clevenger, Ligand-independent dimerization of the human prolactin receptor isoforms: Functional implications. *Mol. Endocrinol.* **20**, 2734–2746 (2006). doi: 10.1210/me.2006-0114; pmid: 16840534
10. E. E. Matthews *et al.*, Thrombopoietin receptor activation: Transmembrane helix dimerization, rotation, and allosteric modulation. *FASEB J.* **25**, 2234–2244 (2011). doi: 10.1096/fj.10-178673; pmid: 21402716
11. O. Livnah *et al.*, An antagonist peptide-EPO receptor complex suggests that receptor dimerization is not sufficient for activation. *Nat. Struct. Biol.* **5**, 993–1004 (1998). doi: 10.1038/2965; pmid: 9808045
12. P. J. Lupardus *et al.*, Structural snapshots of full-length Jak1, a transmembrane gp130/IL-6/IL-6Rα cytokine receptor complex, and the receptor-Jak1 holocomplex. *Structure* **19**, 45–55 (2011). doi: 10.1016/j.str.2010.10.010; pmid: 21220115
13. Single-letter abbreviations for the amino acid residues are as follows: A, Ala; C, Cys; D, Asp; E, Glu; F, Phe; G, Gly; H, His; I, Ile; K, Lys; L, Leu; M, Met; N, Asn; P, Pro; Q, Gln; R, Arg; S, Ser; T, Thr; V, Val; W, Trp; and Y, Tyr.
14. M. Funakoshi-Tago, S. Pelletier, H. Moritake, E. Parganas, J. N. Ihle, Jak2 FERM domain interaction with the erythropoietin receptor regulates Jak2 kinase activity. *Mol. Cell. Biol.* **28**, 1792–1801 (2008). doi: 10.1128/MCB.01447-07; pmid: 18160720
15. X. Lu, L. J. Huang, H. F. Lodish, Dimerization by a cytokine receptor is necessary for constitutive activation of JAK2V617F. *J. Biol. Chem.* **283**, 5258–5266 (2008). doi: 10.1074/jbc.M707125200; pmid: 18158285
16. K. He *et al.*, Janus kinase 2 determinants for growth hormone receptor association, surface assembly, and signaling. *Mol. Endocrinol.* **17**, 2211–2227 (2003). doi: 10.1210/me.2003-0256; pmid: 12920237
17. D. Langosch, B. Brosig, H. Kolmar, H. J. Fritz, Dimerisation of the glycophorin A transmembrane segment in membranes probed with the ToxR transcription activator. *J. Mol. Biol.* **263**, 525–530 (1996). doi: 10.1006/jmbi.1996.0595; pmid: 8918935
18. W. Ruan, V. Becker, U. Klingmüller, D. Langosch, The interface between self-assembling erythropoietin receptor transmembrane segments corresponds to a membrane-spanning leucine zipper. *J. Biol. Chem.* **279**, 3273–3279 (2004). doi: 10.1074/jbc.M309311200; pmid: 14602718
19. S. N. Constantinescu *et al.*, Ligand-independent oligomerization of cell-surface erythropoietin receptor is mediated by the transmembrane domain. *Proc. Natl. Acad. Sci. U.S.A.* **98**, 4379–4384 (2001). doi: 10.1073/pnas.081069198; pmid: 11296286
20. A. N. Bader *et al.*, Homo-FRET imaging as a tool to quantify protein and lipid clustering. *ChemPhysChem* **12**, 475–483 (2011). doi: 10.1002/cphc.201000801; pmid: 21344588
21. S. Ghosh, S. Saha, D. Goswami, S. Bilgrami, S. Mayor, Dynamic imaging of homo-FRET in live cells by fluorescence anisotropy microscopy. *Methods Enzymol.* **505**, 291–327 (2012). doi: 10.1016/B978-0-12-388448-0.00024-3; pmid: 22289460
22. R. S. Kasai *et al.*, Full characterization of GPCR monomer-dimer dynamic equilibrium by single molecule imaging. *J. Cell Biol.* **192**, 463–480 (2011). doi: 10.1083/jcb.201009128; pmid: 21300851
23. L. G. J. Tertoolen *et al.*, Dimerization of receptor protein-tyrosine phosphatase alpha in living cells. *BMC Cell Biol.* **2**, 8 (2001). doi: 10.1186/1471-2121-2-8; pmid: 11401727
24. G. Jiang *et al.*, Dimerization inhibits the activity of receptor-like protein-tyrosine phosphatase-alpha. *Nature* **401**, 606–610 (1999). doi: 10.1038/44170; pmid: 10524630
25. G. Jiang, J. den Hertog, T. Hunter, Receptor-like protein tyrosine phosphatase α homodimerizes on the cell surface. *Mol. Cell. Biol.* **20**, 5917–5929 (2000). doi: 10.1128/MCB.20.16.5917-5929.2000; pmid: 10913175
26. K. F. Kubatzky *et al.*, Structural requirements of the extracellular to transmembrane domain junction for erythropoietin receptor function. *J. Biol. Chem.* **280**, 14844–14854 (2005). doi: 10.1074/jbc.M411251200; pmid: 15657048
27. L. Guan, F. D. Murphy, H. R. Kaback, Surface-exposed positions in the transmembrane helices of the lactose permease of *Escherichia coli* determined by intermolecular thiol cross-linking. *Proc. Natl. Acad. Sci. U.S.A.* **99**, 3475–3480 (2002). doi: 10.1073/pnas.052703699; pmid: 11904412
28. Y. Zhang, J. Jiang, J. J. Kopchick, S. J. Frank, Disulfide linkage of growth hormone (GH) receptors (GHR) reflects GH-induced GHR dimerization. Association of JAK2 with the GHR is enhanced by receptor dimerization. *J. Biol. Chem.* **274**, 33072–33084 (1999). doi: 10.1074/jbc.274.46.33072; pmid: 10551877
29. S. N. Behncken *et al.*, Growth hormone (GH)-independent dimerization of GH receptor by a leucine zipper results in constitutive activation. *J. Biol. Chem.* **275**, 17000–17007 (2000). doi: 10.1074/jbc.275.22.17000; pmid: 10828073
30. T. K. Kerppola, Design and implementation of bimolecular fluorescence complementation (BiFC) assays for the visualization of protein interactions in living cells. *Nat. Protoc.* **1**, 1278–1286 (2006). doi: 10.1038/nprot.2006.201; pmid: 17406412
31. P. Duquesnoy *et al.*, A single amino acid substitution in the exoplasmic domain of the human growth hormone (GH) receptor confers familial GH resistance (Laron syndrome) with positive GH-binding activity by abolishing receptor homodimerization. *EMBO J.* **13**, 1386–1395 (1994). pmid: 8137822

32. E. Biener-Ramanujan, V. K. Ramanujan, B. Herman, A. Gertler, Spatio-temporal kinetics of growth hormone receptor signaling in single cells using FRET microscopy. *Growth Horm. IGF Res.* **16**, 247–257 (2006). doi: 10.1016/j.ghir.2006.06.001; pmid: 16950496
33. G. Skiniotis, P. J. Lupardus, M. Martick, T. Walz, K. C. Garcia, Structural organization of a full-length gp130/LIF-R cytokine receptor transmembrane complex. *Mol. Cell* **31**, 737–748 (2008). doi: 10.1016/j.molcel.2008.08.011; pmid: 18775332
34. J. Staerk *et al.*, An amphipathic motif at the transmembrane-cytoplasmic junction prevents autonomous activation of the thrombopoietin receptor. *Blood* **107**, 1864–1871 (2006). doi: 10.1182/blood-2005-06-2600; pmid: 16249382
35. M. J. Waters, H. N. Hoang, D. P. Fairlie, R. A. Pelekanos, R. J. Brown, New insights into growth hormone action. *J. Mol. Endocrinol.* **36**, 1–7 (2006). doi: 10.1677/jme.1.01933; pmid: 16461922
36. L. Monticelli *et al.*, The MARTINI coarse-grained force field: Extension to proteins. *J. Chem. Theory Comput.* **4**, 819–834 (2008). doi: 10.1021/ct700324x
37. L. Janosi, A. Prakash, M. Doxastakis, Lipid-modulated sequence-specific association of glycophorin A in membranes. *Biophys. J.* **99**, 284–292 (2010). doi: 10.1016/j.bpj.2010.04.005; pmid: 20655857
38. J. Hénin, A. Pohorille, C. Chipot, Insights into the recognition and association of transmembrane α-helices. The free energy of α-helix dimerization in glycophorin A. *J. Am. Chem. Soc.* **127**, 8478–8484 (2005). doi: 10.1021/ja050581y; pmid: 15941282
39. A. Prakash, L. Janosi, M. Doxastakis, GxxxG motifs, phenylalanine, and cholesterol guide the self-association of transmembrane domains of ErbB2 receptors. *Biophys. J.* **101**, 1949–1958 (2011). doi: 10.1016/j.bpj.2011.09.017; pmid: 22004749
40. S. Özdirekcan, D. T. Rijkers, R. M. Liskamp, J. A. Killian, Influence of flanking residues on tilt and rotation angles of transmembrane peptides in lipid bilayers. A solid-state ^{2}H NMR study. *Biochemistry* **44**, 1004–1012 (2005). doi: 10.1021/bi0481242; pmid: 15654757
41. D. Poger, A. E. Mark, Turning the growth hormone receptor on: Evidence that hormone binding induces subunit rotation. *Proteins* **78**, 1163–1174 (2010). doi: 10.1002/prot.22636; pmid: 19927328
42. C. Chen, R. Brinkworth, M. J. Waters, The role of receptor dimerization domain residues in growth hormone signaling. *J. Biol. Chem.* **272**, 5133–5140 (1997). doi: 10.1074/jbc.272.8.5133; pmid: 9030580
43. B. Bernat, G. Pal, M. Sun, A. A. Kossiakoff, Determination of the energetics governing the regulatory step in growth hormone-induced receptor homodimerization. *Proc. Natl. Acad. Sci. U.S.A.* **100**, 952–957 (2003). doi: 10.1073/pnas.0235023100; pmid: 12552121
44. P. van Kerkhof, M. Smeets, G. J. Strous, The ubiquitin-proteasome pathway regulates the availability of the GH receptor. *Endocrinology* **143**, 1243–1252 (2002). doi: 10.1210/endo.143.4.8755; pmid: 11897680
45. O. Silvennoinen, J. N. Ihle, J. Schlessinger, D. E. Levy, Interferon-induced nuclear signalling by Jak protein tyrosine kinases. *Nature* **366**, 583–585 (1993). doi: 10.1038/366583a0; pmid: 7504785
46. I. S. Lucet *et al.*, The structural basis of Janus kinase 2 inhibition by a potent and specific pan-Janus kinase inhibitor. *Blood* **107**, 176–183 (2006). doi: 10.1182/blood-2005-06-2413; pmid: 16174768
47. R. M. Bandaranayake *et al.*, Crystal structures of the JAK2 pseudokinase domain and the pathogenic mutant V617F. *Nat. Struct. Mol. Biol.* **19**, 754–759 (2012). doi: 10.1038/nsmb.2348; pmid: 22820988
48. X. Lu, A. W. Gross, H. F. Lodish, Active conformation of the erythropoietin receptor: Random and cysteine-scanning mutagenesis of the extracellular juxtamembrane and transmembrane domains. *J. Biol. Chem.* **281**, 7002–7011 (2006). doi: 10.1074/jbc.M512638200; pmid: 16414957
49. N. Seubert *et al.*, Active and inactive orientations of the transmembrane and cytosolic domains of the erythropoietin receptor dimer. *Mol. Cell* **12**, 1239–1250 (2003). doi: 10.1016/S1097-2765(03)00389-7; pmid: 14636581
50. J. Staerk *et al.*, Orientation-specific signalling by thrombopoietin receptor dimers. *EMBO J.* **30**, 4398–4413 (2011). doi: 10.1038/emboj.2011.315; pmid: 21892137
51. E. Ishizaka-Ikeda, R. Fukunaga, W. I. Wood, D. V. Goeddel, S. Nagata, Signal transduction mediated by growth hormone receptor and its chimeric molecules with the granulocyte colony-stimulating factor receptor. *Proc. Natl. Acad. Sci. U.S.A.* **90**, 123–127 (1993). doi: 10.1073/pnas.90.1.123; pmid: 7678333
52. P. Saharinen, O. Silvennoinen, The pseudokinase domain is required for suppression of basal activity of Jak2 and Jak3 tyrosine kinases and for cytokine-inducible activation of signal transduction. *J. Biol. Chem.* **277**, 47954–47963 (2002). doi: 10.1074/jbc.M205156200; pmid: 12351625
53. F. Giordanetto, R. T. Kroemer, Prediction of the structure of human Janus kinase 2 (JAK2) comprising JAK homology domains 1 through 7. *Protein Eng.* **15**, 727–737 (2002). doi: 10.1093/protein/15.9.727; pmid: 12456871
54. W. Guo, L. Shi, M. Filizola, H. Weinstein, J. A. Javitch, Crosstalk in G protein-coupled receptors: Changes at the transmembrane homodimer interface determine activation. *Proc. Natl. Acad. Sci. U.S.A.* **102**, 17495–17500 (2005). doi: 10.1073/pnas.0508950102; pmid: 16301531
55. D. Abankwa, H. Vogel, A FRET map of membrane anchors suggests distinct microdomains of heterotrimeric G proteins. *J. Cell Sci.* **120**, 2953–2962 (2007). doi: 10.1242/jcs.001404; pmid: 17690305

Acknowledgments: This work was supported by grants from the National Health and Medical Research Council of Australia (511120, 1002893, and 102082) and the Australian Research Council to M.J.W., A.J.B, A.E.M., and M.W.P. Infrastructure funding from the Victorian Government to St Vincent's Institute is gratefully acknowledged. W.D. and M.D. acknowledge financial support by the NSF (USA) Chemical, Bioengineering, Environmental, and Transport Systems Division (grant number 1067356) and central processing unit time by the University of Houston Research Computing Center. G.A.G. acknowledges financial support by the Kids Cancer Project of the Oncology Research Foundation. We thank W. A. Johnston for optimizing the *Leishmania*-based cell-free lysate expression system used in the single-molecule and Alpha screen interaction studies. Confocal imaging was performed at the IMB/ACRF Cancer Biology Imaging Facility, established with the support of the Australian Cancer Research Foundation.

Supplementary Materials

www.sciencemag.org/content/344/6185/1249783/suppl/DC1
Materials and Methods
Supplementary Text
Figs. S1 to S9
References (*56*–*87*)

16 December 2013; accepted 1 April 2014
10.1126/science.1249783